JOURNAL OF MATERIALS SCIENCE 19 (1984) 3640–3648

The study of model polydiacetylene/epoxy composites

Part 1 *The axial strain in the fibre*

C. GALIOTIS, R. J. YOUNG, P. H. J. YEUNG, D. N. BATCHELDER*
*Department of Materials, and *Department of Physics, Queen Mary College, Mile End Road, London E1 4NS, UK*

A mode composite system consisting of one polydiacetylene single crystal fibre in an epoxy resin matrix has been subjected to tensile strain parallel to the fibre direction. The strain at all points along the length of the fibre was determined by resonance Raman spectroscopy while that of the matrix was measured by conventional techniques. Comparison of the fibre and matrix strain showed two distinct regions. Below about 0.5% matrix strain the composite followed Reuss-type behaviour with equal stress in the fibre and the matrix. At higher matrix strain the composite followed Voigt-type behaviour with any increase in matrix strain matched by an equal increase in fibre strain. In this region the strain distribution along the length of the fibre could be approximately described by the shear-lag model of Cox. The critical length of the fibre was found to increase linearly with fibre diameter as predicted by that model. Good qualitative agreement was found with the predictions of a calculation based on finite element analysis over the full range of applied stress.

1. Introduction

It is well established that the composites produced by incorporating brittle high-modulus fibres in a matrix of epoxy resin or metal can have outstanding mechanical properties. This led to their use initially in the high-technology aerospace industry but now they are finding use in more general engineering applications. Many fibres, such as those of glass, carbon or Kevlar, are produced in continuous form but others are available only as short filaments or whiskers and even continuous fibres are often employed as chopped strands, for example, when they are incorporated into moulding compounds. When discontinuous fibres are used the attainment of good mechanical properties depends critically upon the efficiency of stress transfer between the matrix and fibres.

This problem of stress transfer has received considerable attention over the years and the model system usually considered has been that of a single fibre embedded within a matrix under stress. This system has been analysed from a theoretical viewpoint by several workers [1–3] and also experimentally using photoelastic stress analysis [4–6]. In his classical study, Cox [1] determined analytically both the tensile stresses in the fibre and the shear stresses at the fibre/matrix interface. The relatively simple equations which resulted have made this a very attractive model for numerous applications. The Cox anaysis is, unfortunately, based upon an oversimplified model and includes certain assumptions which are not valid in most composites. For example, the model assumes that no tensile stress is transferred from the matrix to the fibre through adhesion at the ends. There have been attempts to find better analytical solutions but the results obtained do not differ greatly from the Cox analysis except at the fibre ends [2]. An approach of potentially greater usefulness is the application of finite element analysis. Using this technique Carrara and McGarry [3] have been able to determine the effect of fibre-end geometry upon the distribution of stresses in the fibre and the matrix.

0022–2461/84 $03.00 + .12

The leading experimental approach to the problem has been the use of photoelastic analysis to determine the stresses in a birefringent matrix, such as an epoxy resin, containing a single reinforcing fibre. Although this technique gives only the matrix stresses it has been found that the shear stresses near the fibre ends are generally higher than given by the Cox shear-lag model. The results of these experiments are in better agreement with the predictions of more sophisticated analytical solutions [2] and finite element analysis [3]. The photoelastic technique does not, however, allow the variation of tensile stress along the fibre to be determined. This is unfortunate since the strength of composites is often limited by fibre fracture in regions of high fibre tensile stress.

Polydiacetylene (PDA) fibres have promising mechanical properties with values of Young's modulus up to 65 GPa and strengths over 1.5 GPa in the fibre direction [7]; the modulus perpendicular to the fibre axis is considerably smaller. As the single crystal fibres also show no creep and have good thermal stability they have considerable potential as reinforcing fibres in all-polymer composites. The resonance Raman (RR) spectrum of a PDA crystal usually has only four to six intense lines, one of which has a frequency of about 2100 cm^{-1} and corresponds to a vibrational mode dominated by stretching of the triple bond [8]. When tensile stress is applied to the crystal along the direction of the polymer chain this Raman line has been found to shift to lower frequency at a rate of approximately 20 cm^{-1} for a 1% strain [9]. In the present study we have used RR spectroscopy to directly measure the point-to-point variation in strain along a polydiacetylene single crystal fibre embedded in an epoxy resin matrix which was under an applied tensile stress. In this circumstance the fibres behave as if they have an internal molecular strain gauge [10]. It has been possible to determine both the efficiency of stress transfer in the PDA fibre/epoxy resin system and, more generally, to investigate the fundamental mechanisms of reinforcement in fibre composites.

2. Experimental procedure

The substituted diacetylene derivative 1,6-di-(*N*-carbazolyl)-2,4-hexadiyne (DCH) was prepared by previously described techniques [11, 12]. Monomer crystals with their axial dimension much longer than their transverse dimension were prepared by slow evaporation from toluene solution. The axial direction corresponded to the crystallographic *b*-axis and the single crystals had facets corresponding to the (1 0 0), (1 0 2) and ($\bar{1}$ 0 2) planes [13]. The ends of the fibre were also faceted, the crystallographic planes involved all intersecting the *b*-axis at angles of greater than 70°. The diameter of the approximately cylindrical crystals could be controlled in the 10 to 100 μm range by adjusting the rate of crystallization; the length varied between 5 and 30 mm. Crystals of uniform diameter and free of obvious surface defects were polymerized by exposure to 35 to 40 Mrad of ^{60}Co γ-radiation. As a result of the topochemical reaction, the polymer chains (pDCH) formed parallel to the long axis thus creating single crystal polymer fibres. The fibres had a Young's modulus of 45 ± 1 GPa in the axial direction [14].

Single fibre composite specimens were prepared with Ciba-Geigy XD 927 two-part solvent-free cold-setting epoxy using (by weight) 100 parts of resin to 36 of hardener. It had been previously demonstrated that pDCH fibres bond well to an epoxy resin [10]. For these experiments it was also important that the epoxy matrix should be sufficiently transparent and free from fluorescence that RR spectra could be measured for embedded fibres. The PTFE mould was half filled with epoxy and allowed to partially set before the fibre and the rest of the epoxy were added. This ensured that the fibre was approximately at the centre of the 6 mm thick specimen. The results for specimens prepared in this way were the same as for those prepared by the more difficult technique of introducing the fibre into the already filled mould. After setting at room temperature for 24 h, thin-film resistance strain gauges of gauge factor 2.1 were attached with the same epoxy to the surface of the specimen at the centre of the fibre. With a DVM it was possible to measure the matrix strain to an absolute accuracy of ± 0.05%. On two specimens strain gauges were placed at various positions on the surface to confirm that the matrix strain was uniform over the full length of the fibre. The finished specimens were cured at 100° C for a further 16 h and then polished to give smooth transparent surfaces. Holes were drilled at both ends to acommodate the clamps used to apply tensile stress; a typical specimen is shown in Fig. 1. After completion of the measurements the specimens were sectioned at several points to determine the fibre diameter. Dummy specimens

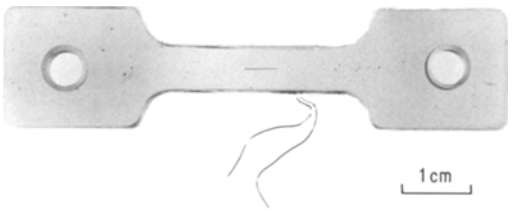

Figure 1 Single fibre composite specimen. The pDCH fibre is located at the centre of the specimen while the resistive strain gauge is attached to the outer surface.

without fibres were subjected to standard tensile test procedures to determine the mechanical properties of the epoxy resin matrix. The Young's modulus of 2.8 ± 0.3 GPa was in reasonable agreement with the prediction of the manufacturer.

A small tensile loading device was used to apply stress in the fibre direction. The device was mounted on a micrometer slide so that the full length of the fibre could be traversed through the incident laser beam. The RR spectra were measured with 180° backscattering geometry using a double monochromator and photon counting system [15] with the 676 nm line of a Kr ion laser. The laser beam intensity was approximately 5 mW and the focal spot was about 25 μm diameter; under these conditions there was no risk of damaging the crystal while good positional sensitivity was retained. The 2085 cm^{-1} Raman line of the pDCH single crystal fibres could be measured with an accuracy of ± 2 cm^{-1}; shifts in the frequency could usually be measured with greater precision. Prior to undertaking the composite experiments the shift of this line with tensile strain had been measured for a DCH fibre which was gripped at the ends but otherwise free-standing [16]. The data shown in Fig. 2 were very similar to those found for other PDA single crystal fibres [9, 17, 18]; for pDCH fibres the Raman frequency was found to decrease at 19.7 ± 0.4 cm^{-1}/% for tensile strain. Thus measurement of the RR spectrum of a fibre under tensile stress made it possible to determine the strain within a 25 μm diameter region on the fibre to an absolute accuracy of about ± 0.1%. The RR technique measures the strain at the surface of the pDCH fibre since the effective skin depth for Raman scattering at this wavelength is only about 10 nm [15].

3. Results and discussion

3.1. Strain at the fibre midpoint

Fig. 3 shows the axial strain at the midpoint of pDCH fibre I in a composite specimen similar to that in Fig. 1 as a function of the strain in the epoxy resin matrix when uniaxial tensile stress was applied to the specimen. The strain in the embedded fibre was determined by the frequency of the Raman line, that of the matrix by the attached resistive strain gauge. Thus the matrix strain referred to in this paper is that in the bulk of the specimen which in general will be different from the local strain of the matrix in the vicinity of the fibre. The 4.5 mm long fibre had a diameter of 21 μm. Below 0.5% matrix strain the data follow the Reuss line (R) in Fig. 3 which has been predicted by assuming that the stresses in the fibre and matrix are equal [19]. Since the modulus of the fibre is approximately 16 times that of the matrix its strain under these conditions is expected to be considerably less than that of matrix. At matrix strains above 1%, however, additional strain in the matrix is matched by that in the fibre. Thus in Fig. 3, the data is parallel to the Voigt line (V), which was drawn using the assumption that the strain in the fibre and matrix are equal [19]. There

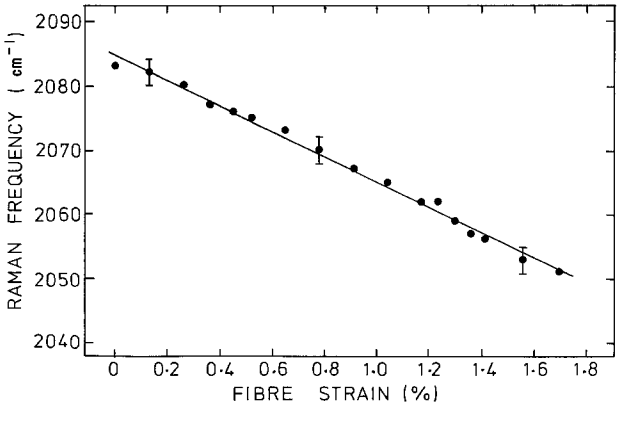

Figure 2 Strain dependence of the 2085 cm^{-1} Raman line of a free-standing pDCH fibre.

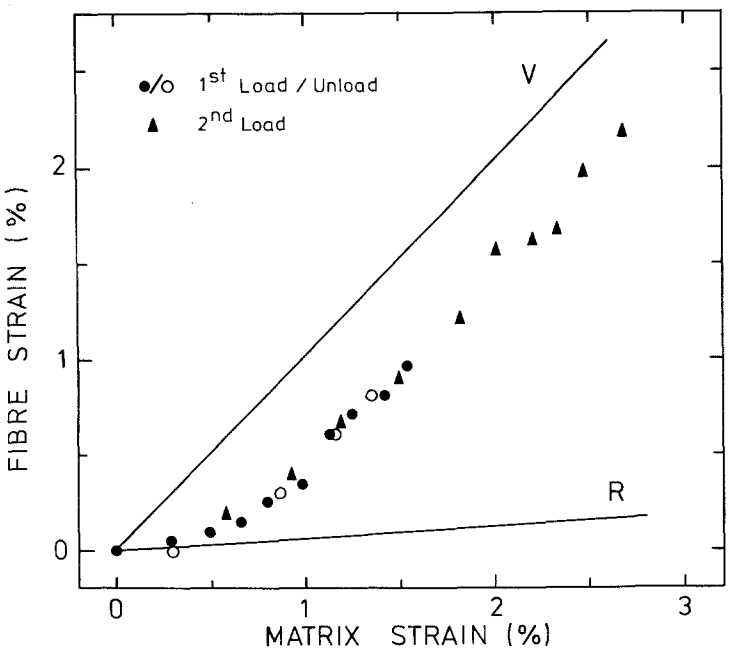

Figure 3 Axial strain at the midpoint of fibre I as a function of matrix strain.

was no hysteresis observed in the strain of fibre and matrix when the specimen was unloaded and then reloaded. There was some residual strain in both fibre and matrix which remained after the applied tensile stress had been removed; this will be discussed below. Similar results are shown in Fig. 4 for pDCH fibre II which was 72 μm diameter and 9.0 mm long. Very little hysteresis was observed between the fibre and matrix strains even after four loadings.

For different fibres of a wide variety of diameters and lengths we have attempted to define the point at which a specimen enters the high strain region. This was done by plotting the data as in Figs. 3 and 4, fitting a straight line of unit slope to the high strain data and extrapolating back to zero fibre strain. The intercept with the horizontal axis has been defined as the critical matrix strain; this is a measure of the matrix strain at which the specimen enters the region of Voigt-type behav-

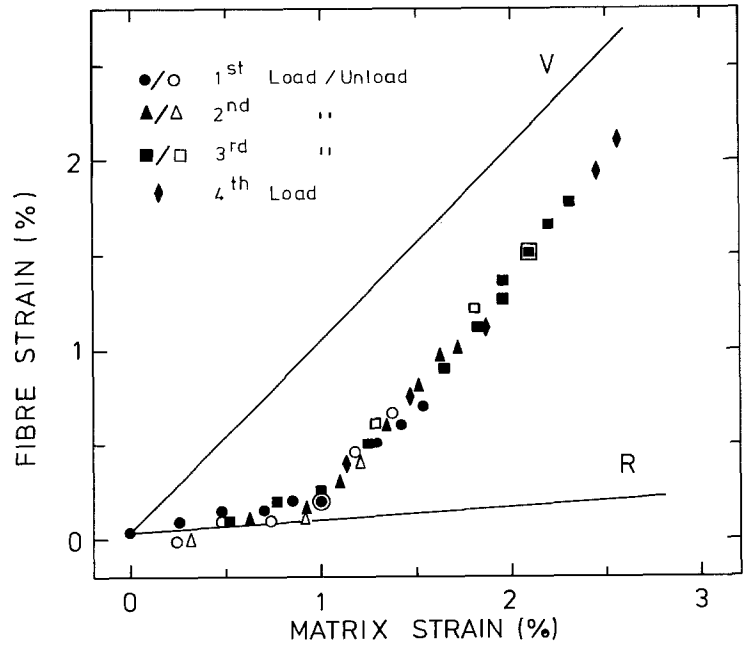

Figure 4 Axial strain at the midpoint of fibre II as a function of matrix strain.

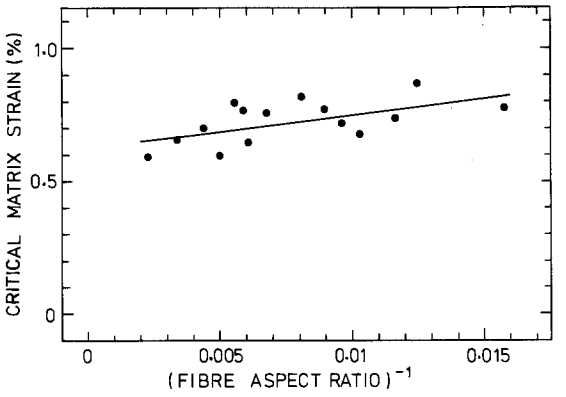

Figure 5 Critical matrix strain for 15 different single fibre composite specimens plotted as a function of the inverse of the aspect ratio of the fibres.

iour. The results plotted in Fig. 5 show that the critical matrix strain is nearly independent of the fibre aspect ratio and hence must be essentially a property of the matrix.

3.2. Distribution of strain along the fibre

The strain distributions along fibres I and II are shown in Figs. 6 and 7 respectively for several different matrix strains. Up to 1% matrix strain there appears to be a uniform strain along the entire length of the fibres. This is to be expected if, as suggested by Figs. 3 and 4, the fibre and matrix are under conditions of equal stress in the low strain region. At higher matrix strains the strain at the end of the fibre saturates while that in the central portion continues to increase in proportion to the matrix strain. As shown in Fig. 6 the length over which the fibre strain rises from its value at the end to that of the central section is equivalent to half the "critical length", l_c. The fibre length must be greater than l_c if the saturation value of the axial strain is to be reached at the midpoint. This length is closely related to the critical length determined by fibre pull-out tests [20–22]. On the fourth loading, fibre II was taken to such high stress that debonding of the end of the fibre occurred. This is shown by the essentially zero strain over the first 0.5 mm of the fibre in Fig. 7c. This was the only instance in which there was an indication that the bonding between fibre and matrix was anything other than perfect; all other specimens suffered matrix fracture before debonding occurred. A fibre treated with epoxy release agent before it was embedded in the matrix was not subject to any axial strain when the matrix was stressed. This showed that frictional forces were insignificant as compared to those arising from adhesion for this polydiacetylene/epoxy composite.

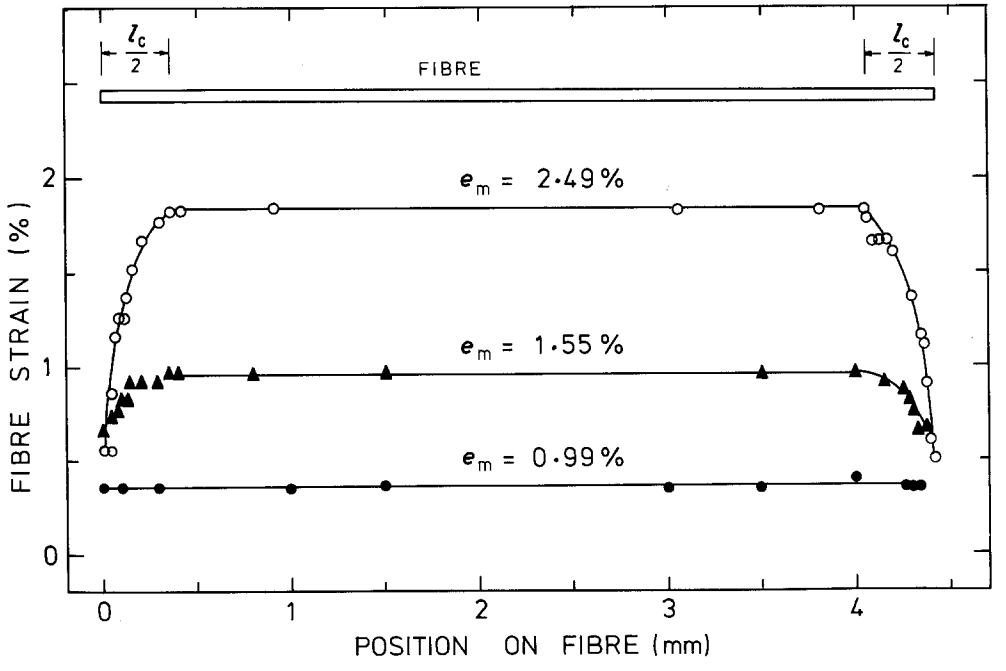

Figure 6 Axial strain of fibre I as a function of the position along the fibre.

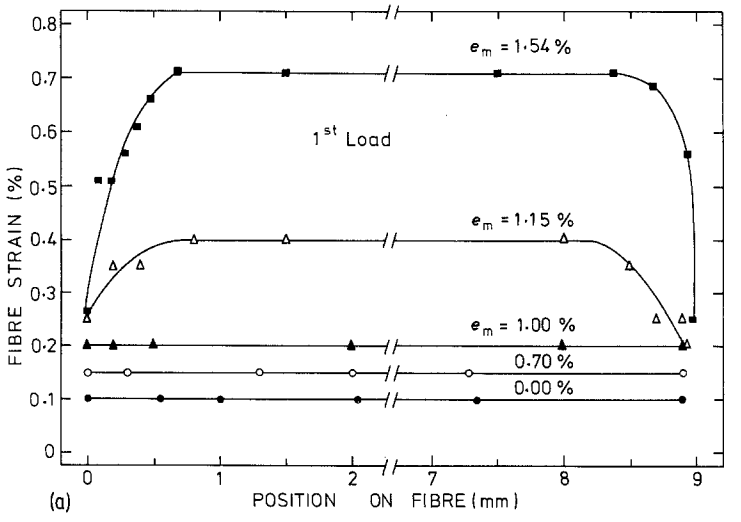

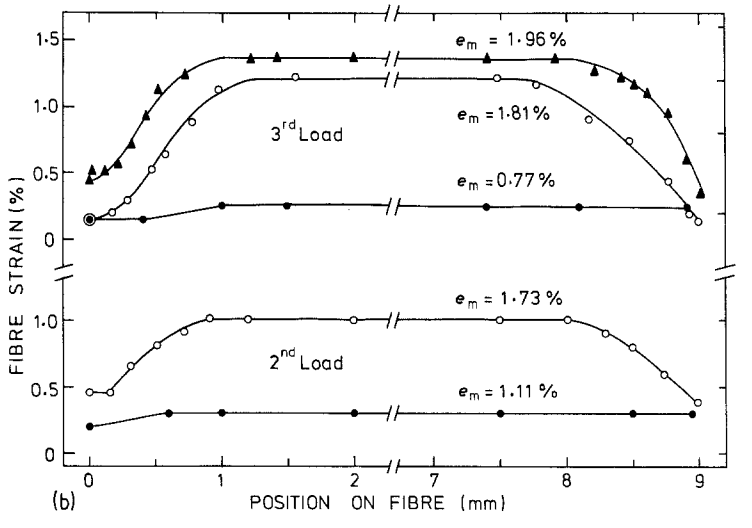

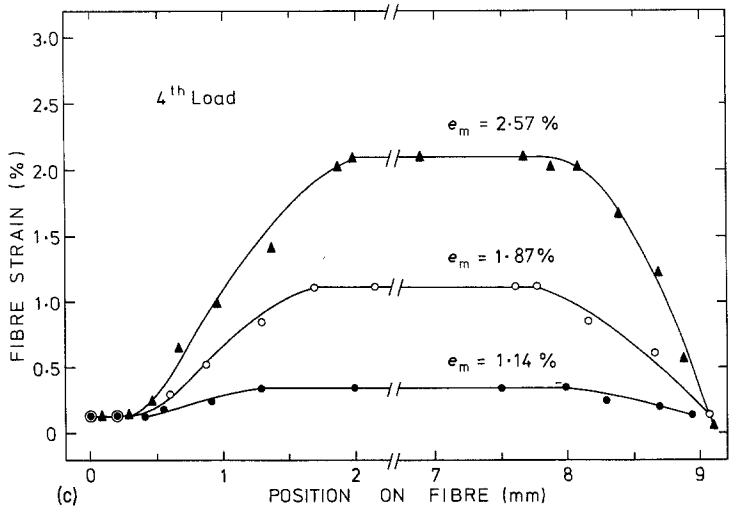

Figure 7 Axial strain of fibre II as a function of the position along the fibre: (a) first loading, (b) second and third loadings, and (c) fourth loading.

3.3. Mechanism of stress transfer

Figs. 3 and 4 show that in the low strain region ($< 0.5\%$) the composite follows Reuss-type behaviour and the axial strain in the fibre is primarily determined by the stress placed upon the fibre through the matrix attachment at the ends. Thus the stress in the fibre is uniform along its length and approximately equal to the stress in the matrix. The fibre modulus is much greater than that of the matrix so its corresponding strain is much less though also uniform along the length of the fibre. Figs. 6 and 7 demonstrate both of these features. For matrix strains over 1%, the high strain region, the relative displacement of the fibre and matrix causes a concentration of shear stresses in the matrix in the vicinity of the fibre ends. These shear stresses in the matrix are converted into tensile stresses in the fibre at the fibre/matrix interface as first pointed out by Cox [1]. In this way "grips" are formed on the end of the fibre and additional tensile stresses in the matrix are transferred through them. Thus in the high strain region the additional strains in fibre and matrix are equal and the shear-lag model of Cox should be in at least qualitative agreement with the results of the present experiment. Since the shear-lag model assumes no stress is transferred through adhesion at the ends of the fibre it can make no predictions about the behaviour of a specimen in the low strain region.

The Cox model is not strictly applicable to the single fibre composite since it assumes that the composite contains many fibres. The approach remains very attractive, however, since it gives a simple analytical solution. The predictions of the model for the relation between axial fibre strain, ϵ_f, and matrix strain, ϵ_m, in the high strain region can be summarized in the single equation

$$\epsilon_f/\epsilon_m = 1 - \frac{\cosh (L/2 - x)/l_0}{\cosh L/2l_0} \qquad (1)$$

where x is the position along a fibre of length L. The constant l_0 is given by

$$l_0 = r\left[\frac{E_f \ln (R/r)}{2G_m}\right]^{1/2}, \qquad (2)$$

where E_f is the tensile modulus of the fibre, G_m the shear modulus of the matrix, r the fibre radius and R the separation between fibres. Predictions for the behaviour of a single fibre composite could in principle be made by letting $R \to \infty$. Unfortunately, the cylindrical symmetry of the problem produces the term $[\ln (R/r)]^{1/2}$ in Equation 2. Although this term is a very slowly varying function for large values of the ratio R/r, equal to 1.5 for $R/r = 10$ and 3.7 for $R/r = 10^6$, it does ultimately lead to a logarithmic divergence for the single fibre composite. Thus comparisons between the present results and the predictions of the Cox model can only be done on a qualitative basis.

For $L \gg 1$ Equation 1 can be simplified to the following form:

$$\epsilon_f/\epsilon_m = 1 - \exp [-x/l_0] - \exp [-(L-x)/l_0]. \qquad (3)$$

It can be seen that for positions well away from the fibre ends $\epsilon_f = \epsilon_m$, while ϵ_f decays exponentially to zero as the fibre ends are approached, reaching the $1/e$ point at $x = l_0$ or $x = L - l_0$. Thus the constant l_0 can be identified as roughly equivalent to half the critical length l_c determined in the present experiments. For large values of R/r, therefore, Equation 2 predicts that l_0 should be directly proportional to the fibre diameter. The results of measurements of l_c for 17 pDCH fibres of differing diameter are shown in Fig. 8. The data points almost all fall on the straight line passing through the origin within their uncertainty limits, and so agree very well with that prediction. The logarithmic divergence in Equation 2 makes it impossible, however, to compare the slope of the line in Fig. 8 with that predicted by the Cox model.

The proportionality of l_c and r can also be predicted without recourse to any specific model of fibre and matrix. For a single fibre in an infinite matrix we would expect, purely on the grounds of dimensional analysis, that l_c should be scaled with respect to r for a given L/r ratio, where L is the total length of the fibre. This implies the existence of a functional relationship between the two dimensionless quantities which can be expressed as $l_c/r = f(L/r)$. This function f should smoothly approach a constant value as $L/r \to \infty$, that is as each end of the fibre becomes effectively one end of a semi-infinite fibre. Therefore, for sufficiently large L/r the constancy of the function f implies that l_c/r must also attain a constant value.

The finite element analysis of Carrara and McGarry [3] was carried out on single fibre composite specimens of similar elastic properties to the present specimens although it was assumed that the fibres as well as the matrix possessed elastic isotropy. Fig. 8 of that paper, in which the axial

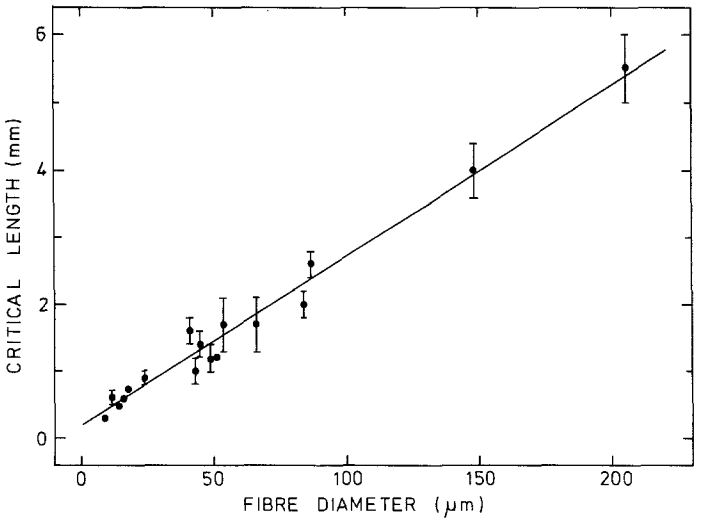

Figure 8 Critical length, l_c, determined for 17 different pDCH fibres in the same way as illustrated for fibre I in Fig. 5, plotted as a function of the fibre diameter.

stress is plotted as a function of position along the fibre, shares two features in common with Figs. 6 and 7 in the present paper, in which axial strain is plotted as a function of position. The axial stress and strain in the fibre are simply related by the Young's modulus of the fibre so the two types of plot are equivalent. Firstly, the finite element analysis shows that the axial stress in the fibre rises from a finite value at the end of the fibre to a fairly constant value of the central portion of the fibre. Secondly, the axial stress at the midpoint of the fibre is lower than that applied to the matrix. Unfortunately, the finite element analysis is a numerical procedure without an analytical solution. Thus it is not possible to compare the present results quantitatively with those of Carrara and McGarry. It is clear, however, that this approach contains the basic elements necessary to explain the results of the present experiments.

3.4. Residual matrix strain

When the stress applied to a specimen was removed the matrix strain as determined by the attached strain gauge initially remained infinite. The magnitude of this residual matrix strain increased until a limiting value was reached. The applied stress at which the limit was reached was essentially the same as that required to take the composite specimen in the high strain region where additional matrix and fibre strains were equal. As shown in Fig. 5, the critical matrix strain required to reach the high strain region was nearly independent of the aspect ratio of the embedded fibre and hence must be largely determined by the matrix alone. This property of the matrix would thus appear to be an important factor in the formation of the "grips" which mark the transition to the Voigt-type behaviour. It was also found that this residual strain relaxed over a period of several days as shown by the results for a single specimen in Fig. 9. This suggests that the very high shear stresses that lead to the formation of the "grips" take the matrix into a deformed state from which it is difficult to recover. This slow return to elastic behaviour could be described as viscoelastic.

3.5. Future work

The results of the measurements of the axial strain of the pDCH fibre in the model composite suggested a number of further projects which are currently in progress. The stresses in the matrix are to be studied by the photoelastic technique so that a more complete picture of the fibre/matrix interaction can be obtained. Finite element analysis will then be carried out on a model which is a

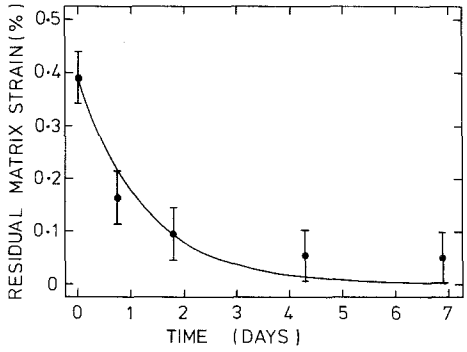

Figure 9 Residual matrix strain for a typical specimen as a function of the time elapsed after the removal of the tensile stress.

close approximation to the present system so that the validity of this approach can be quantitatively tested. Finally, the transition from Reuss to Voigt behaviour will be studied as a function of the volume fraction of fibres.

4. Conclusions

It has been demonstrated that it is possible to measure the axial strain in a PDA single crystal fibre in a transparent epoxy resin matrix. For matrix strains below 0.5%, the single fibre model composite demonstrated Reuss-type behaviour with the axial stress approximately equal to the tensile stress in the matrix. Above 1% matrix strain, the application of additional tensile stress resulted in Voigt-type behaviour with the tensile strain in the fibre matching that in the matrix. In the high strain region the simple model of Cox provides a qualitative description which can explain most of the observed results. An approach such as that supplied by finite element analysis, however, will be required to give a quantitative description over the full range of applied stress.

Acknowledgements

The authors are grateful to Mr I. F. Chalmers and Dr D. Bloor for supplying the DCH monomer and to Dr P. Clay of Imperial College for the γ-ray polymerization of the fibres. We are grateful to the reviewer for suggesting the dimensional argument for the constancy of l_c/r. The work was supported by grants from the Science and Engineering Research Council and the US Army through its European Research Office.

References

1. H. L. COX, *Brit. J. Appl. Phys.* **3** (1952) 72.
2. G. E. SMITH and A. J. M. SPENCER, *J. Mech. Phys. Solids* **18** (1970) 81.
3. A. S. CARRARA and F. J. McGARRY, *J. Comp. Mater.* **2** (1968) 222.
4. D. M. SCHUSTER and E. SCALA, *Trans. Metal. Soc.* **230** (1964) 1635.
5. W. R. TYSON and G. W. DAVIES, *Brit. J. Appl. Phys.* **16** (1965) 199.
6. I. M. ALLISON and L. C. HOLLOWAY, *ibid.* **18** (1967) 979.
7. C. GALIOTIS and R. J. YOUNG, *Polymer* **24** (1983) 1023.
8. W. F. LEWIS and D. N. BATCHELDER, *Chem. Phys. Lett.* **60** (1979) 232.
9. D. N. BATCHELDER and D. BLOOR, *J. Polymer Sci. Polymer Phys. Ed.* **17** (1979) 569.
10. C. GALIOTIS, R. J. YOUNG and D. N. BATCHELDER, *J. Mater. Sci. Lett.* **2** (1983) 236.
11. V. ENKELMANN, G. SCHEIER, G. WEGNER, H. EICHELE and M. SCHWOERER, *Chem. Phys. Lett.* **52** (1977) 314.
12. K. C. YEE and R. R. CHANCE, *J. Polymer Sci. Polymer Phys. Ed.* **16** (1978) 431.
13. V. ENKLEMANN, R. J. LEYRER, G. SCHLEIER and G. WEGNER, *J. Mater. Sci.* **15** (1980) 168.
14. C. GALIOTIS, R. T. READ, P. H. J. YEUNG, R. J. YOUNG, I. F. CHALMERS and D. BLOOR, *J. Polymer Sci. Polymer Phys. Ed.* in press.
15. D. N. BATCHELDER and D. BLOOR, in "Advances in Infrared and Raman Spectroscopy", Vol. 11, edited by R. J. H. Clark and R. E. Hester (Wiley Heydon, Chichester, 1983) p. 133.
16. C. GALIOTIS, Ph.D. thesis, University of London (1982).
17. V. J. MITRA, W. M. RISEN, Jr and R. H. BAUGHMAN, *J. Chem. Phys.* **66** (1977) 2731.
18. C. GALIOTIS, R. J. YOUNG and D. N. BATCHELDER, *J. Polymer Sci. Polymer Phys. Ed.* **21** (1983) 2483.
19. R. P. KAMBOUR and R. E. ROBERTSON, "Polymer Science", edited by A. D. Jenkins (North-Holland, London, 1972) p. 687.
20. C. C. CHAMIS, in "Composite Materials", Vol. 6, edited by E. P. Plueddeman (Academic Press, New York, 1974) p. 31.
21. P. BARTOS, *J. Mater. Sci.* **15** (1980) 2133.
22. N. H. LADIZESKY and I. M. WARD, *ibid.* **18** (1983) 533.

Received 16 November 1983
and accepted 24 January 1984